Development of porous ceramics with well-controlled porosities and pore sizes from apatite fibers and their evaluations

M. KAWATA, H. UCHIDA, K. ITATANI, I. OKADA, S. KODA
Department of Chemistry, Faculty of Science and Engineering, Sophia University, 7-1, Kioi-cho, Chiyoda-ku, Tokyo, Japan 102-8554

M. AIZAWA*
Department of Industrial Chemistry, Faculty of Science and Technology, Meiji University, 1-1-1 Higashi-Mita Tama-ku Kawasaki-shi, Kanagawa, Japan 214-8571
E-mail: mamorua@isc.meiji.ac.jp

Porous hydroxyapatite (HAp) ceramics possessing well-controlled porosities and pore sizes were developed by firing apatite-fiber compacts mixed with carbon beads and agar. The total porosities could be controlled in the range from 40 to 85% by varying compaction pressure (20–40 MPa), firing temperature (1000–1300 °C) and carbon/HAp ratio (0/10–10/10 (w/w)). Most of the pores were regarded as open pores. The pore sizes were mainly affected by the carbon-bead diameter (5, 20 or 150 μm) and partly by the compaction pressure and the firing temperature. The pore sizes of the porous HAp ceramics derived from the carbon beads of 150 μm in diameter were distributed in the two separate ranges of several micrometers and more than 100 μm.

1. Introduction

Since hydroxyapatite ($Ca_{10}(PO_4)_6(OH)_2$; HAp) is a chief inorganic material present in vertebrate's hard tissues, and has excellent biocompatibility, it is used also as a substitute material for human hard tissues [1, 2]. HAp materials are commercially available in the shapes of granules [3], dense ceramics [4, 5] and porous ceramics [6, 7]. Among them, the porous ceramics have attracted much attention on applications to tissue engineering [8] and drug delivery systems [9]. The physical and biological properties of the porous ceramics strongly depend on their porosities and pore sizes. Therefore, both the porosities and the pore sizes are required to be well-controlled for the practical applications.

We have previously reported that single-crystal apatite fibers having long-axis sizes from 60 to 100 μm can be prepared by a homogeneous precipitation method through heating of the solution in the $Ca(NO_3)_2$–$(NH_4)_2HPO_4$–$(NH_2)_2CO$–HNO_3–H_2O system [10, 11]; subsequently, porous HAp ceramics with well-controlled open pores were fabricated by sintering these apatite fibers [12]. Most of the pores in the resulting porous ceramics were regarded as the open pores, and the pore sizes could be controlled in the range from 0.2 to 1 μm by varying the compaction pressure and firing temperature; however, larger pores of $\sim$ 100 μm in diameter were not formed.

Furthermore, the porous HAp ceramics derived from the apatite fibers were applied to the matrices of the HAp/PMMA (polymethylmethacrylate) hybrid materials [13–15]: the hybrid materials were fabricated by introducing methylmethacrylate (MMA) into the open pores of the porous HAp ceramics and by *in situ* polymerization of MMA to PMMA inside the pores. The mechanical properties of the resulting hybrid materials were $\sim$ 63 GPa in Young's modulus, $\sim 2\,MPa\,m^{1/2}$ in the fracture toughness (K_{IC}) and $\sim$ 65 MPa in the bending strength [13, 14]. These values were similar to those of the living cortical bone. The hybrid materials have the excellent cellular responses with respect to the cell proliferation, the differentiation and the better *in vivo* tissue reaction in the rabbit model than that of the dense HAp ceramics [14, 15].

The fracture toughness will be enhanced, when the open pores of the ceramics are enlarged enough and into which biocompatible polymers can be introduced. Further, using biodegradable polymers [16, 17] (PLLA, PGA and their co-polymer) instead of PMMA, we can also design hard-tissue substituting hybrid materials which integrate with host bone.

In order to develop the above hybrid materials, we need to fabricate HAp ceramics having pores of large size. The main aim of the present study was to control the porosities and the pore sizes of porous HAp ceramics derived from the apatite fibers by the present newly

*Author to whom all correspondence should be addressed.

developed process using carbon beads and agar. Such porous HAp ceramics must be effective for the matrices of hybrid materials, as well as for the filters of water purification, the carriers of enzymes and microorganisms as bioreactors [18, 19].

2. Materials and methods

2.1. Fabrication of porous HAp ceramics

As previously reported [12], single-crystal apatite fibers were prepared by a homogeneous precipitation method from the solution in the $Ca(NO_3)_2$–$(NH_4)_2HPO_4$–$(NH_2)_2CO$–HNO_3–H_2O system. The starting solution of the Ca/P ratio of 1.67 was prepared by mixing $Ca(NO_3)_2$, $(NH_4)_2HPO_4$, $(NH_2)_2CO$ and HNO_3 to be 0.167, 0.100, 0.500 and 0.10 mol dm^{-3} aqueous solutions, respectively. The solution was heated at 80 °C for 24 h and then 90 °C for 72 h to synthesize apatite fibers having long-axis sizes from 60 to 100 μm.

The resulting apatite fibers were suspended in water, so that the concentration was $\sim$ 1 wt %. Carbon beads (Nikabeads; Nihon Carbon Company) of 5, 20 or 150 μm in average diameter were added to the apatite-fiber slurry in the following carbon/HAp ratios: 0/10, 1/10, 5/10 or 10/10 (w/w). The particle morphologies of these carbon beads are shown in Fig. 1. Then, agar was added to the carbon/HAp-mixed slurry to be at 0.10 wt %. The resulting slurry was heated by using a water bath to dissolve agar, and ethanol was added to the slurry at a ratio of 7/3 (v/v) for water/ethanol. After stirring the slurry, it was allowed to cool to room temperature. The above slurry was poured into aluminum tubes of 10 mm in internal diameter and suction-filtrated to prepare the precursors of green compacts.

After the precursors were air-dried at room temperature, they were uniaxially compressed at 20, 30 or 40 MPa to form the green compacts. The porous HAp ceramics were fabricated by firing the green compacts at 1000, 1100, 1200 or 1300 °C for 5 h in a steam atmosphere; the heating rate was 10 °C min^{-1} and the steam saturated at 30 °C was introduced into the tube-type furnace at a rate of $\sim$600 cm^3 min^{-1} using a compressor. As mentioned above, four fabrication conditions, that is, the compaction pressure, the firing temperature, the carbon/HAp ratio and the carbon-bead diameter, were systematically varied on the processing of the present porous HAp ceramics.

2.2. Evaluation of the porous HAp ceramics

The relative density (d_{rela}) of the resulting porous HAp ceramics is defined by

$$d_{rela} = 100(\rho_{bulk}/\rho_{theo}) \quad (1)$$

where ρ_{bulk} and ρ_{theo} are the bulk density and the theoretical density of the HAp (3.16 g cm^{-3}), respectively.

The total porosity (P_{total}) of the resulting ceramics was evaluated by

$$P_{total} = 100 - d_{rela} \quad (2)$$

The open porosity (P_{open}) and closed porosity (P_{closed})

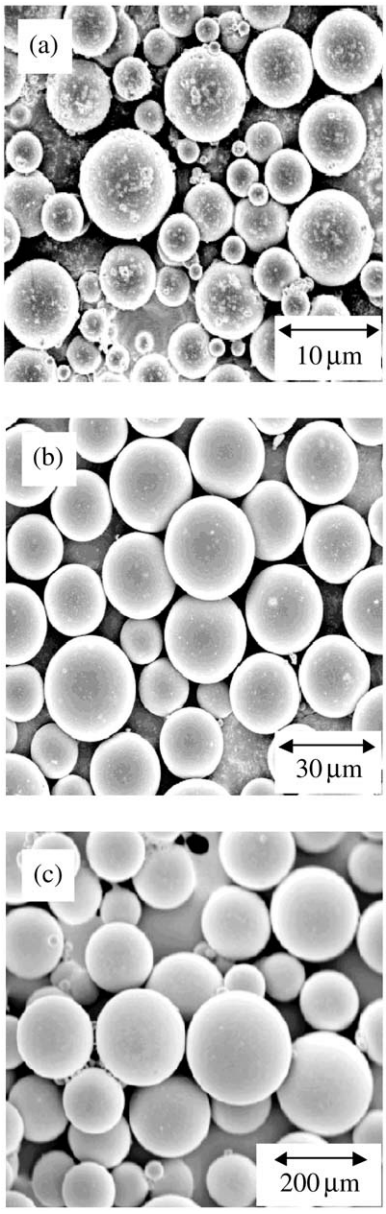

Figure 1 Particle morphologies of the carbon beads used on the processing of the porous HAp ceramics; diameter: (a) 5 μm, (b) 20 μm and (c) 150 μm.

were determined by the apparent density (ρ_{app}) of the resulting ceramics and the theoretical density of the HAp as follows:

$$P_{closed} = 100(1 - (\rho_{app}/\rho_{theo})) \quad (3)$$

$$P_{open} = P_{total} - P_{closed} \quad (4)$$

The ρ_{app} was measured at 25 $\pm$ 0.2 °C using a picnometer, where ethanol was used as an immersion liquid.

The crystalline phases of the resulting ceramics were identified by X-ray diffractometry (XRD; Rigaku Corp., RINT2000PC, 40 kV, 40 mA, CuK_α radiation). The functional groups were detected by Fourier-transform infrared spectroscopy (FT-IR; Shimadzu Corp., 8200D, measurement range: 400–4000 cm^{-1}).

The compressive strength of the resulting porous ceramics was measured using a 500 kgf load cell at a cross-head speed of 0.5 mm min^{-1} (Yasuda Seiki, AUTOSTRAIN YZ-500). The tested specimen was in

the cylindrical shape of ~ 9 mm in diameter and ~ 6 mm in thickness. Six specimens were measured; the average value and the standard deviation were taken as the compressive strength.

The microstructures of the resulting ceramics were observed by scanning electron microscopy (SEM; Hitachi, S4500, 5 kV). The pore size distributions were examined by mercury penetration porosimetry (Shimadzu Corp., micromeritics Pore Sizer 9310).

3. Results and discussion

Fig. 2 shows an XRD pattern (Fig. 2(a)) and an FT-IR spectrum (Fig. 2(b)) of the typical porous ceramics fabricated under the following conditions; the compaction pressure: 30 MPa, the firing temperature: 1200 °C, the carbon/HAp ratio: 5/10 (w/w), the carbon-bead diameter: 150 μm. The powdered porous ceramics were used for the XRD and FT-IR measurements. The XRD pattern reveals that a single phase of HAp was present in the sample. The FT-IR spectrum shows the absorptions at 1300–900, 600 and 570 cm^{-1} assignable to the PO_4^{3-} group, and at 3570 and 630 cm^{-1} due to the OH^- group [20].

The XRD patterns and FT-IR spectra did not appreciably vary by changes in the fabrication conditions. As far as the firing temperature was varied in the range from 1000 to 1300 °C, by-products expected from decomposition of HAp, such as tricalcium phosphate (TCP) and calcium oxide, were not found. The additions of the carbon beads at the carbon/HAp ratio from 0/10 to 10/10 (w/w) had no significant effect on the phase compositions or the functional groups of the porous HAp ceramics; no incorporation of CO_3^{2-} into HAp was detected. The phase compositions and the functional groups of the resulting ceramics did not vary by changes in the compaction pressure or the carbon-bead diameter. The above results show that the porous ceramics fabricated under various fabrication conditions are composed of the HAp single phase containing OH^- group.

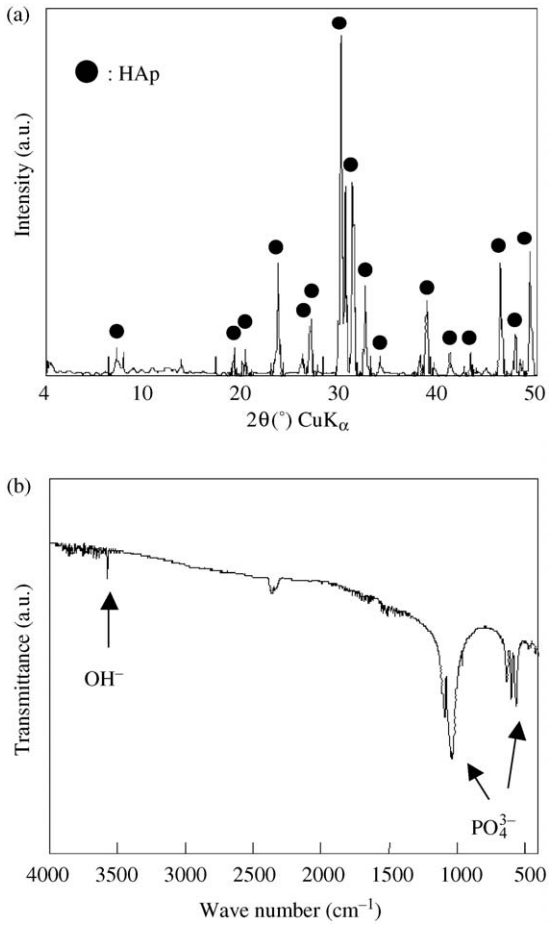

Figure 2 (a) XRD pattern and (b) FT-IR spectrum of the typical porous ceramics fabricated under the following conditions; compaction pressure: 30 MPa, firing temperature: 1200 °C, carbon/HAp ratio: 5/10 (w/w), carbon-bead diameter: 150 μm.

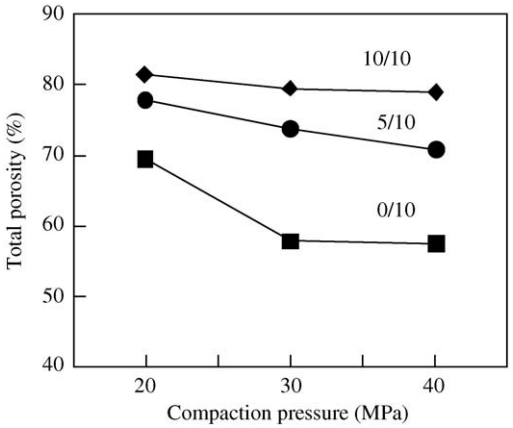

Figure 3 Relationship between compaction pressure and total porosity of the porous HAp ceramics; firing temperature: 1200 °C, carbon/HAp ratio: 0/10, 5/10 and 10/10 (w/w), carbon-bead diameter: 150 μm.

Fig. 3 shows the relationship between compaction pressure and total porosity. The total porosities decreased with increasing compaction pressure. This is due to closer packing of the green compacts with increasing compaction pressure. The total porosities of the porous ceramics fabricated with carbon beads were higher than those without carbon beads.

Fig. 4 shows the relationship between firing temperature and total porosity. The total porosities decreased with increasing firing temperature; especially, the porosity of the porous ceramics fabricated without carbon beads attained about 40% at 1300 °C. On the other hand, in the case of the porous ceramics fabricated

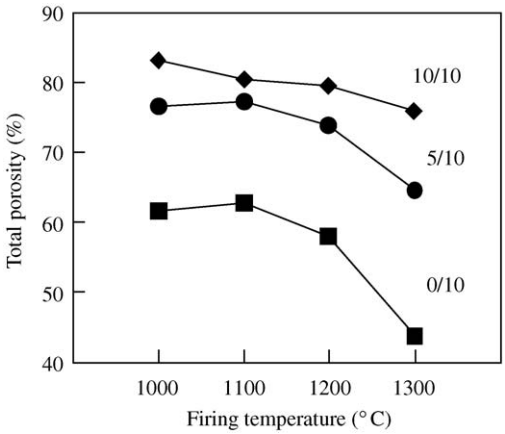

Figure 4 Relationship between firing temperature and total porosity of the porous HAp ceramics; compaction pressure: 30 MPa, carbon/HAp ratio: 0/10, 5/10 and 10/10 (w/w), carbon-bead diameter: 150 μm.

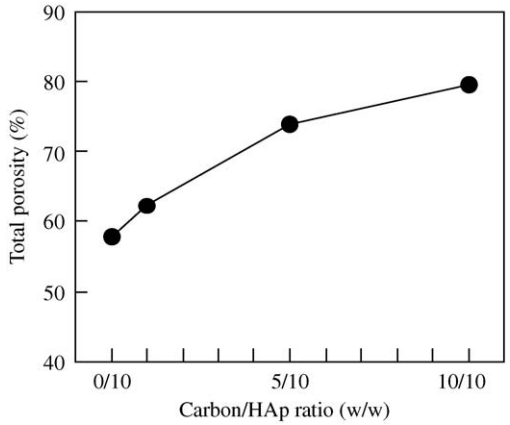

Figure 5 Changes in the total porosities of the porous HAp ceramics with the carbon/HAp ratio (carbon-bead content in the apatite-fiber green compacts); compaction pressure: 30 MPa, firing temperature: 1200 °C, carbon-bead diameter: 150 μm.

with carbon beads, the porosities attained the high values in the range from 80 to 85%. The decrease in the total porosities with increasing firing temperature is due to promotion of the sintering.

Fig. 5 shows the changes in the total porosities with the carbon/HAp ratio (carbon-bead content in the apatite-fiber green compacts). The total porosities increased with the carbon-bead content. This phenomenon is occurred by the pore formations due to the burning-out of the carbon beads during the sintering. The carbon-bead diameter had no significant effect on the total porosities.

The results of the porosities thus demonstrate that the total porosities can be controlled in the range from 40 to 85% by varying fabrication conditions, such as the compaction pressure (20–40 MPa), the firing temperature (1000–1300 °C) and the carbon/HAp ratio (0/10–10/10 (w/w)). The total porosities of the ceramics decreased with increasing compaction pressure and firing temperature; this can be interpreted in terms of the densification of the ceramics during the sintering. The total porosities increase with the carbon-bead content, because the carbon beads are burned-out during the sintering to form pores of large size.

Further, proportions of open to closed porosities in the resulting porous ceramics were also investigated. Table I gives the porosities of the typical porous HAp ceramics fabricated under the four conditions given there. The closed porosities of the porous ceramics measured using a picnometer were less than 10% in almost all the porous ceramics fabricated under various conditions. In other words, most of the present porous ceramics were composed of the open pores. These results indicate that the present porous ceramics have been developed in the interconnected 3-D structures inside the ceramics.

Table II gives the compressive strengths of the typical porous HAp ceramics. The total porosities of these specimens were constant at $\sim 70\%$. These low compressive strengths are reasonable in the light of the high total porosities of $\sim 70\%$.

Fig. 6 shows the microstructures of the resulting porous ceramics fabricated under the conditions given in Table I; the fabrication conditions for Fig. 6(a)–(d) correspond to those for Specimens (A), (B), (C) and (D), respectively, in Table I, and Fig. 6(a′), (b′), (c′) and (d′) are the magnified ones of Fig. 6(a), (b), (c) and (d), respectively.

Fig. 6(a) and (a′) show the microstructures of the porous ceramics fabricated without carbon beads. These reveal that the microstructures are uniform, and are composed of the sintered fibers and the micro-pores of 1–2 μm.

Fig. 6(b)–(d′) correspond to the microstructures of the porous ceramics fabricated with carbon beads. Whereas the total porosities of these specimens are nearly constant at $\sim 75\%$ as given in Table I, each microstructure considerably differs from sample to sample depending on the carbon-bead diameter. These microstructures were composed of sintered fibers and many pores which are classified as the macro-pores of more than ~ 10 μm and the micro-pores of less than 1–2 μm. The macro-pore sizes increase with the carbon-bead diameter; on the other hand, the micro-pore sizes are practically independent of the carbon-bead diameter. As previously stated, no macro-pores were formed without use of the carbon-beads.

These SEM observations suggest that the macro-pores were formed by the burning-out of the carbon beads, while the micro-pores by the intertwining followed by bonding of individual fibers during the sintering.

TABLE I Porosities of typical porous HAp ceramics

Specimen	Compaction pressure (MPa)	Firing temperature (°C)	Carbon/HAp ratio (w/w)	Carbon-bead diameter (μm)	P_{total} (%)	P_{closed} (%)	P_{open} (%)	$\frac{P_{closed} \times 100}{P_{total}}$
(A)	30	1200	0/10	—	57.9	5.4	52.5	9.3
(B)	30	1200	5/10	5	76.0	3.1	72.9	4.1
(C)	30	1200	5/10	20	73.1	2.1	71.0	2.9
(D)	30	1200	5/10	150	73.9	8.3	65.6	11.2

TABLE II Compressive strengths of typical porous HAp ceramics

Specimen	Compaction pressure (MPa)	Firing temperature (°C)	Carbon/HAp ratio (w/w)	Carbon-bead diameter (μm)	P_{total} (%)	Compressive strength (MPa)
(E)	40	1300	10/10	5	73.1 ± 0.5	1.7 ± 0.3
(F)	40	1300	10/10	20	68.4 ± 0.3	3.1 ± 0.3
(G)	40	1300	10/10	150	73.4 ± 0.4	1.0 ± 0.2

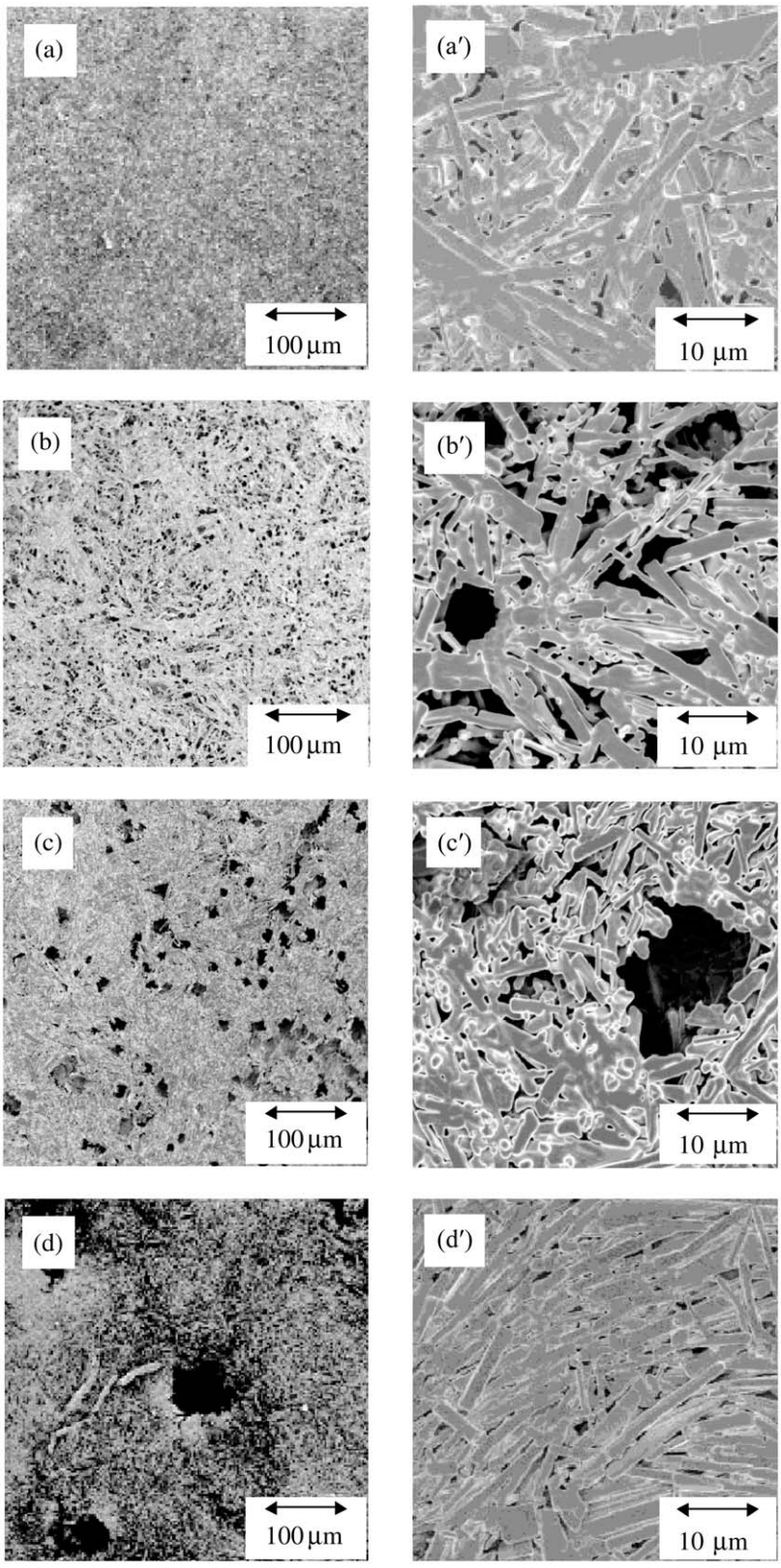

Figure 6 Microstructures of the porous HAp ceramics. As for the fabrication conditions, see the text.

Therefore, we consider from these results that the macropore sizes of the present porous ceramics can be controlled just by selecting the diameter of the carbon beads with their total porosities kept constant.

Furthermore, the porous structure of the ceramics was examined by a mercury penetration porosimeter. Fig. 7 shows the distributions of the pore sizes of the porous HAp ceramics fabricated under the same conditions as those of the SEM observations. Among the above-mentioned four fabrication conditions, the carbon-bead diameter has most significantly affected the pore sizes.

As shown in Fig. 7(a), the pore size distribution of the porous ceramics fabricated without carbon beads showed a normal distribution curve centered on $\sim 1\,\mu m$. This median pore size is 1.2 μm. The addition of the carbon beads enlarged the pore sizes of the specimens; the median pore sizes are 2.5, 2.6 and 5.4 μm when the

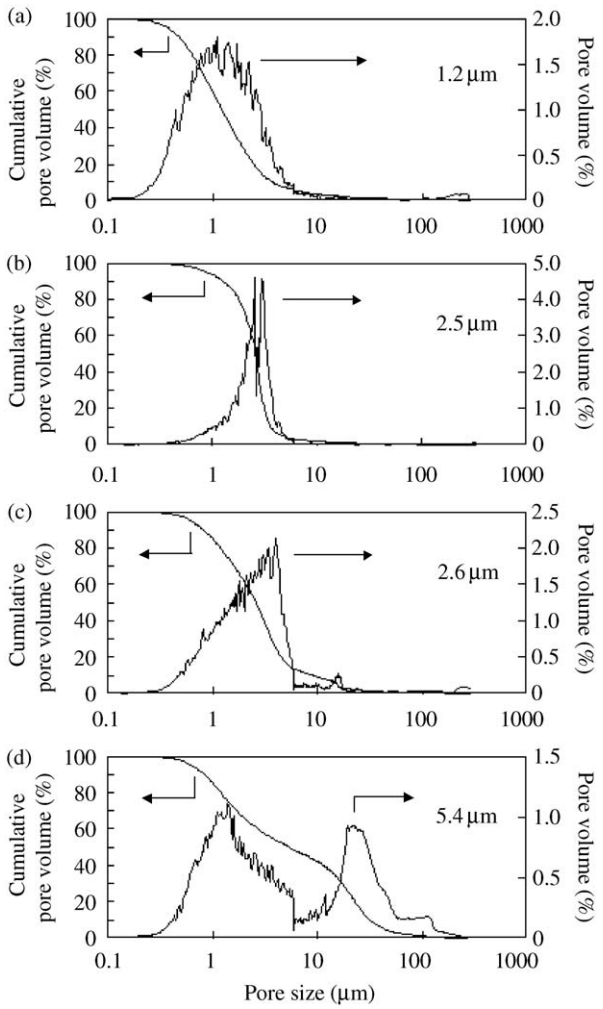

Figure 7 Pore size distributions of the porous HAp ceramics. As for the fabrication conditions, the present (a), (b), (c) and (d) correspond to Specimens (A), (B), (C) and (D), respectively, in Table I. The median pore sizes are also given in the figure.

carbon beads are 5, 20 and 150 μm, respectively, in diameter. In other words, with increasing carbon-bead diameter, the median pore size enlarged; this result is consistent with that obtained by the SEM observations.

When the carbon beads of 150 μm in diameter were used, the pore size distribution was separated into two ranges. It is generally known that the tissue reactions of the ceramics implanted in the bone are largely influenced by both micro- and macro-pores [21]. Therefore, the present porous ceramics possessing bi-modal pore size distributions may be considered to have ideal micro-structures as the substitute materials for human hard tissues.

Thus, novel processing of porous HAp ceramics having well-controlled porosities and micro/macro-pore sizes could be established using single-crystal apatite fibers mixed with carbon beads of various diameters and agar.

Such porous HAp ceramics can be expected to be useful in many fields. For example, the above porous HAp ceramics will be used as the matrices of the HAp/polymer hybrid materials to improve the mechanical properties and to investigate the relationship between the mechanical properties and the pore sizes. In addition, such porous HAp ceramics may be effective as a novel matrix for tissue engineering of human hard tissue [7, 22, 23], the filters for water purification and the carriers of enzymes and microorganisms for bioreactors [18, 19].

4. Conclusion

Porous HAp ceramics have been fabricated from single-crystal apatite fibers prepared by a homogeneous precipitation method. The results obtained are summarized as follows:

1. The total porosities could be controlled in the range from 40 to 85% by varying the compaction pressure (20–40 MPa), the firing temperature (1000–1300 °C) and the carbon/HAp ratio (0/10–10/10 (w/w)).
2. The pore sizes chiefly depended on the carbon-bead diameter (5, 20 and 150 μm); that is, only the pore sizes can be changed with their porosities kept constant just by varying the carbon-bead diameter.

The present investigation demonstrates that the porosities and the pore sizes could be simultaneously controlled by varying the fabrication conditions, that is, the compaction pressure, the firing temperature, the carbon/HAp ratio and the carbon-bead diameter. Thus, we have established the new process using carbon beads and agar.

References

1. L. L. HENCH, *J. Am. Ceram. Soc.* **81** (1998) 1705.
2. T. KOKUBO, H.-M. KIM and M. KAWASHITA, *Bull. Ceram. Soc. Japan* **38** (2003) 2.
3. N. PETAL, I. R. GIBSON, K. A. HING, S. M. BEST, E. DAMIEN, P. A. REVELL and W. BONFIELD, *Key Eng. Mater.* **218–220** (2002) 383.
4. R. Z. LEGEROS and J. P. LEGEROS, in ''An Introduction to Bioceramics'' (World Scientific, Singapore, 1993) p. 139.
5. M. AIZAWA, T. HANAZAWA, K. ITATANI, F. S. HOWELL and A. KISHIOKA, *J. Mater. Sci.* **34** (1999) 2865.
6. E. C. SHORS and R. E. HOLMES, in ''An Introduction to Bioceramics'' (World Scientific, Singapore, 1993) p. 181.
7. V. S. KOMLEV and M. BARINOV, *J. Mater. Sci.: Mater. Med.* **13** (2002) 295.
8. H. OGUSHI, *J. Biomed. Mater. Res.* **48** (1999) 913.
9. M. AIZAWA, H. SHINODA, H. UCHIDA, K. ITATANI, I. OKADA, M. MATSUMOTO, H. MORISUE, H. MATSUMOTO and Y. TOYAMA, *Key Eng. Mater.* **240–242** (2003) 647.
10. M. KINOSHITA, A. KISHIOKA, H. HAYASHI and K. ITATANI, *Gypsum & Lime* **219** (1989) 79.
11. M. AIZAWA, F. S. HOWELL, K. ITATANI, Y. YOKOGAWA, K. NISHIZAWA, M. TORIYAMA and T. KAMEYAMA, *J. Ceram. Soc. Jpn.* **108** (2000) 249.
12. M. AIZAWA, A. PORTER, S. BEST and W. BONFIELD, *Key Eng. Mater.* **240–242** (2003) 509.
13. M. AIZAWA, Y. TSUCHIYA, K. ITATANI, H. SUEMASU, A. NOZUE and I. OKADA, *Bioceramics* **12** (1999) 453.
14. M. AIZAWA, M. ITO, K. ITATANI, H. SUEMASU, A. NOZUE, I. OKADA, M. MATSUMOTO, M. ISIKAWA, H. MATSUMOTO and Y. TOYAMA, *ibid.* **14** (2001) 465.
15. M. AIZAWA, M. ITO, K. ITATANI, I. OKADA and M. MATSUMOTO, *Phosphorus Lett.* **46** (2003) 7.
16. M. KUSANO, M. SUGIMURA, K. NOMURA and K. NISHIMURA, *J. Maxill. Biomech.* **1** (1995) 47.
17. M. KUSANO, M. SUGIMURA, K. NOMURA and K. NISHIMURA, *ibid.* **1** (1995) 61.
18. T. TATEISHI and A. ITO, *Bull. Ceram. Soc. Japan* **28** (1993) 631.

19. S. HIRATA, K. MATSUMOTO and H. OHYA, *Gypsum & Lime* **240** (1992) 364.
20. B. O. FOWLER, E. C. MORENO and W. E. BROWN, *Arch. Oral. Biol.* **11** (1966) 477.
21. H. YOKOZEKI, T. HAYASHI, T. NAKAGAWA, H. KUROSAWA, K. SHIBUYA and K. IOKU, *J. Mater. Sci.: Mater. Med.* **9** (1998) 381.
22. M. AIZAWA, H. UENO and K. ITATANI, *Mater. Integ.* **12** (1999) 75.
23. M. AIZAWA, Japan Pat.: Tokukai #2003-93052.

Received 16 October 2003
and accepted 21 January 2004